Continuous Symmetries and Observability Properties in Autonomous Navigation

Agostino Martinelli

INRIA

INSTITUT NATIONAL DE RECHERCHE EN INFORMATIQUE ET EN AUTOMATIQUE

Continuous Symmetries and Observability Properties in Autonomous Navigation

Agostino Martinelli

N° 7049 — version 2

initial version October 2009 — revised version October 2010

Thèmes COG et NUM

ISSN 0249-6399 ISRN INRIA/RR--7049--FR+ENG

INSTITUT NATIONAL
DE RECHERCHE
EN INFORMATIQUE
ET EN AUTOMATIQUE

INRIA

centre de recherche
GRENOBLE - RHÔNE-ALPES

Continuous Symmetries and Observability Properties in Autonomous Navigation

Agostino Martinelli

Thèmes COG et NUM — Systèmes cognitifs et Systèmes numériques
Équipe-Projet Emotion

Rapport de recherche n° 7049 — version 2 — initial version October 2009 — revised version October 2010 — 32 pages

Abstract: This paper considers the problem of state estimation from a theoretical perspective. In particular, the investigation regards problems where the information provided by the sensor data is not sufficient to carry out the state estimation (i.e. the state is not observable). For these systems it is introduced the concept of continuous symmetry. Detecting the continuous symmetries of a given system has a very practical importance. It allows us to detect an observable state whose components are non linear functions of the original non observable state. This theoretical and very general concept is applied to deal with two distinct fundamental estimation problems in mobile robotics. The former is in the framework of self-calibration and the latter is in the framework of the fusion of the data provided by inertial sensors and vision sensors. For both problems all the observable modes are analytically derived by analyzing the continuous symmetries.

Key-words: State Estimation and Navigation, Sensor Fusion, Localization, Non Observability, Calibration, Mobile Robotics, Aerial Navigation, Inertial and visual data fusion

Centre de recherche INRIA Grenoble – Rhône-Alpes
655, avenue de l'Europe, 38334 Montbonnot Saint Ismier
Téléphone : +33 4 76 61 52 00 — Télécopie +33 4 76 61 52 52

Symétries Continues et Propriétés d'Observabilité dans la Navigation Autonome

Résumé : Ce document considère le problème de l'estimation en robotique mobile depuis un point de vue théorique. Plus précisément on considère situations ou l'information contenue dans le données des capteurs est pas suffisante pour l'estimation (c'est-à-dire l'état n'est pas observable). Pour ces systèmes on introduit le concept de symétrie continue. Détecter les symétries continues d'un tel système est très importante en pratique. Il permet de trouver un nouvel état observable dont les composantes sont fonctions non linéaires de l'état originel. Pour montrer la puissance de ce concept son application á deux problèmes d'estimation très importantes en navigation autonome seront présentés. Le premièr est un problème d'auto calibration pour les capteurs d'un robot mobile en utilisant une seule amère. Le deuxièm est un problèm d'estimation dans le quadre de la fusion entre la vision et les capteurs inertiels.

Mots-clés : Estimation et Navigation, Fusion Sensoriel, Localisation, Non observabilité, Robots Mobiles, Navigation aérien, Fusion de la vision avec les capteurs inertiels, Calibration

1 Introduction

Autonomous navigation requires in many cases to solve simultaneously different tasks (e.g. localization, mapping, obstacle avoidance etc.). Among them, several are estimation tasks, i.e. the robot has to be able to autonomously estimate a given state by integrating the information contained in its sensor data. Typical examples of estimation problems fundamental in many robotics applications are localization, SLAM, calibration, tracking and many others. In all these problems the goal is to estimate a given state starting from the sensor data.

In every estimation problem the following fundamental questions must be answered:

1. Does the system contain the necessary information to perform the estimation of the considered state?

2. In the case the answer to the previous question is negative, is it possible to detect a new state for which the information allows performing the estimation?

The answer to the first question is provided by a well known concept developed in the framework of control theory: the observability. In control theory, a system is defined observable when it is possible to reconstruct its initial state by knowing, in a given time interval, the system inputs and the outputs [4]. The observability properties can be easily derived in a linear system by performing the so called Kalman canonical decomposition (see, e.g., [4]). However, in a non linear system, this concept is much more complex and the observability becomes a local property [7]. In a nonlinear system the concept of *Weak Local Observability* was introduced by Hermann and Krener [7]. The same authors introduced also a criterion, the *observability rank criterion*, to verify whether a system is weak local observable (WLO) in a given point. The application of the rank criterion only requires to perform differentiation and has extensively been adopted in mobile robotics to investigate the observability properties of non linear systems (see section 1.1).

Answering the second question is in general much harder and could be done by using the theory of distributions [9]. When a system is not WLO in any point of the space of the states there are in general infinite possible initial states reproducing exactly the same inputs and outputs. Let us consider for instance the $2D$ localization problem when the robot moves along a corridor and it is equipped with odometry sensors and sensors able to perform relative observations (e.g. bearing and range sensors). Under these hypotheses, all the initial states differing for a shift along the corridor reproduce exactly the same inputs and outputs. Intuitively, we remark that the entire system has one continuous symmetry corresponding to the shift along the corridor. Furthermore, it is obvious that the only quantities that we can estimate (i.e. which are WLO) are invariant with respect to this continuous symmetry (i.e. the robot orientation and the distance of the robot from the corridor walls). The previous consideration regarding this simple localization problem is pretty trivial and does not require to introduce special mathematical tools. However, there are cases where it is a very challenging task answering the second question, i.e. detecting a new WLO state and its link with the data provided by the robot's sensors. The

key and starting point to deal with these cases is to provide a mathematical definition of continuous symmetry.

1.1 Related Works

Regarding the localization problem, the observability analysis has been carried out by several authors. Roumeliotis [20] presented it for a multi robots system equipped with encoder and sensors able to provide an observation consisting of the relative configuration between each pair of robots. The analysis was performed through the linear approximation. The main result of this observability analysis was that the system is not observable and it becomes observable when at least one of the robots in the team has global positioning capabilities. Bonnifait and Garcia considered the case of one robot equipped with encoders and sensors able to provide the bearing angles of known landmarks in the environment [3]. The observability analysis was carried out by linearizing the system (as in the previous case) and by applying the *observability rank condition*. As in many nonlinear systems, they found that in some cases while the associated linearized system is not observable, the system is WLO. Furthermore, Bicchi and collaborators extended the case of a single robot to the SLAM problem ([2], [14]). They considered one robot equipped with the same bearing sensors of the previous case. They considered in the environment landmarks with a priori known position and landmarks whose position has to be estimated. They found that two landmarks are necessary and sufficient to make the system observable. Furthermore, they applied optimal control methods in order to minimize the estimation error. In particular, in [14] they maximized the Cramer-Rao lower bound as defined in [11]. Very recently, the observability rank condition has been adopted to investigate the observability properties for the problem of calibrating a vision sensor [15] [17]. Furthermore, the observability rank criterion has recently been applied to the SLAM problem [8] [13]. Finally, an observability analysis has been performed in order to investigate the properties of the concurrent bias estimation in the map aided localization problem [18].

However, in all these works what it was determined is only whether the state defining the system configuration is WLO or not (i.e. only the first question has been considered).

1.2 Paper Contributions and Paper Structure

In this paper we want to take a step forward whose importance is in our opinion fundamental when dealing with a non observable problem. Indeed, when a state is not WLO, estimating directly the state brings to inconsistency with catastrophic consequences. On the other hand, when a state is not WLO, suitable functions of its components could be WLO and therefore could be estimated. We will call these functions *Observable Modes*. The derivation of the observable modes is fundamental in order to properly perform the estimation.

In this paper we introduce some mathematical tools to derive the observable modes for systems which are not WLO. These mathematical tools are based on the concept of continuous symmetry whose definition is here introduced. This theoretical and very general concept is applied to deal with two distinct fundamental estimation problems in mobile robotics. The former is in the framework of self-calibration and the latter is in the framework of the fusion of the data

provided by inertial sensors (IMU) and vision sensors. For both problems all the observable modes are analytically derived by analyzing the continuous symmetries.

Section 2 provides a very simple example to better illustrate the concept of continuous symmetry. As for the previously mentioned $2D$ localization in a corridor, analytical methods are not required to detect the observable modes due to the simplicity of the chosen example. The theoretical concepts introduced in section 3 will be illustrated by referring to this simple example. In particular, we remind the rank criterion introduced by Hermann and Krener [7] and we introduce the concept of continuous symmetry. Starting from this definition we derive partial differential equations which characterize all the observable modes in a given system. In section 4 the calibration problem will be discussed. In section 5 and 6 the problem of fusing the data from a camera with IMU will be considered. Several results showing the importance of detecting all the observable modes will be provided in section 7.

2 A Simple Example of Localization

We consider a mobile robot moving in a $2D$-environment. The configuration of the robot in a global reference frame can be characterized through the vector $[x_R,\ y_R,\ \theta_R]^T$ where x_R and y_R are the cartesian robot coordinates and θ_R is the robot orientation. The dynamics of this vector are described by the following non-linear differential equations:

$$\begin{cases} \dot{x}_R = v\cos\theta_R \\ \dot{y}_R = v\sin\theta_R \\ \dot{\theta}_R = \omega \end{cases} \tag{1}$$

where v and ω are the linear and the rotational robot speed, respectively. The robot is equipped with proprioceptive sensors able to evaluate these two speeds. We assume that it exists a point feature in our environment and, without loss of generality, we fix the global reference frame on it (see figure $1a$). The robot is also equipped with a bearing sensor (e.g. a camera) able to evaluate the bearing angle of the point feature in its own frame. Therefore, our system has the following output (see fig. $1a$):

$$y = \beta \equiv \pi - \theta_R + atan2(y_R, x_R) \tag{2}$$

We also provide the equations for the same system in polar coordinates, i.e. when the robot configuration is described by the coordinates D, $\phi_R \equiv atan2(y_R, x_R)$ and θ_R.

$$\begin{cases} \dot{D} = v\cos(\theta_R - \phi_R) \\ \dot{\phi}_R = \dfrac{v}{D}\sin(\theta_R - \phi_R) \\ \dot{\theta}_R = \omega \\ y = \pi - \theta_R + \phi_R \end{cases} \tag{3}$$

Our goal is to answer the two questions mentioned in the previous section for the system characterized by the equations (1-2) or (3). Since the system is very simple, we do not need special mathematical tools.

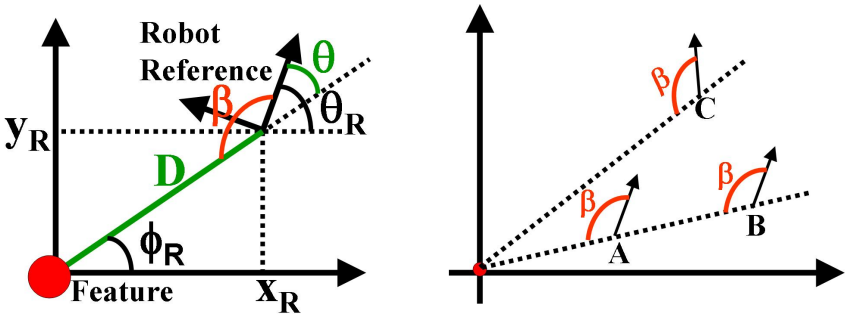

a *b*

Figure 1: A simple localization problem. The robot is equipped with odometry sensors and bearing sensors able to evaluate the angle β. In b the three initial robot configurations are compatible with the same initial observation (β).

To check whether we have the necessary information to estimate the robot configuration $[x_R,\ y_R,\ \theta_R]^T$ we have to prove that it is possible to uniquely reconstruct the initial robot configuration by knowing the input controls and the outputs (observations) in a given time interval. When at the initial time the bearing angle β of the origin is available, the robot can have every position in the plane but for each one only one orientation provides the right angle β. In fig. 1b all the three positions A, B and C are compatible with the observation β provided that the robot orientation satisfies (2). In particular, the orientation is the same for A and B but not for C.

Let us suppose that the robot moves according to the inputs $v(t)$ and $\omega(t)$. With the exception of the special motion consisting of a line passing by the origin, by only performing a further bearing observation it is possible to distinguish all the points belonging to the same line passing by the origin. In fig. 2a the two initial positions in A and B do not reproduce the same observations ($\beta_A \neq \beta_B$). On the other hand, all the initial positions whose distance from the origin is the same cannot be distinguished independently of the chosen trajectory. In fig. 2b the two indicated trajectories provide the same bearing observations at every time. Therefore, the dimension of the undistinguishable region is 1 and the dimension of the largest WLO subsystem is $3 - 1 = 2$.

We remark that the system has a continuous symmetry: the system inputs ($v(t)$ and $\omega(t)$) and outputs ($y(t)$) are invariant with respect to a rotation of the global frame about the vertical axis (in the next section we will provide a mathematical definition for a general continuous symmetry). From the fact that the dimension of the largest WLO subsystem is two, we know that we can only estimate two independent modes. Furthermore, these two modes must satisfy the previous system invariance, i.e. they must be rotation invariant. A possible choice is provided by the two quantities D and θ in figure 1 ($\theta \equiv \theta_R - atan2(y_R, x_R)$).

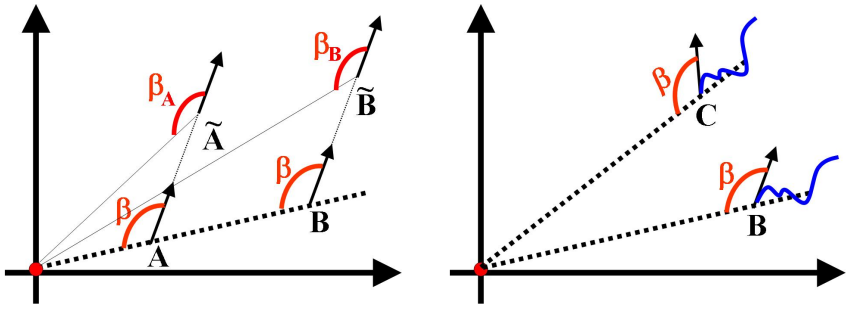

a *b*

Figure 2: In a the two initial positions (A and B) do not reproduce the same observations ($\beta_A \neq \beta_B$). In b the two indicated trajectories provide the same bearing observations at every time.

The new system is characterized by the following equations:

$$\begin{cases} \dot{D} = v\cos\theta \\ \dot{\theta} = \omega - \dfrac{v}{D}\sin\theta \\ y = \pi - \theta \end{cases} \tag{4}$$

which express the link between the new state $[D,\ \theta]^T$ and the proprioceptive data $(v,\ \omega)$ and the exteroceptive data (β).

The detection of the previous two modes and the derivation of the equations in (4) is fundamental (i.e the answer to the second question stated in the introduction). Indeed, estimating the original state brings to inconsistency with catastrophic consequences. In the next section we want to provide some mathematical tools in order to perform the same analysis. This will allow us to answer the two questions stated in the introduction for more complicated estimation problems in the framework of autonomous navigation.

3 Continuous Symmetries and Observability Properties

A general characterization for systems in the framework of autonomous navigation is provided by the following two equations describing respectively the dynamics and the observation:

$$\begin{cases} \dot{S} = f(S,u) = f_0(S) + \sum_{i=1}^{M} f_i(S)u_i \\ y = h(S) \end{cases} \tag{5}$$

where $S \in \Sigma \subseteq \Re^n$ is the state, $u = [u_1,\ u_2,\ ...,\ u_M]^T$ are the system inputs, $y \in \Re$ is the output (we are considering a scalar output for the sake of clarity, the extension to a multi dimensions output is straightforward). Both the systems defined by (1-2) or (3) and the one defined by (4) can be characterized by (5).

For instance, for the system in (3) we have: $S = [D,\ \phi_R,\ \theta_R]^T$, $f_0 = [0, 0, 0]^T$, $M = 2$, $u_1 = v$, $u_2 = \omega$, $f_1(S) = [\cos(\theta_R - \phi_R),\ \frac{\sin(\theta_R - \phi_R)}{D},\ 0]^T$, $f_2(S) = [0,\ 0,\ 1]^T$, $h(S) = \pi - \theta_R + \phi_R$.

3.1 Observability Rank Criterion

We want to remind some concepts in the theory by Hermann and Krener in [7]. We will adopt the following notation. We indicate the k^{th} order Lie derivative of a field Λ along the vector fields $v_{i_1}, v_{i_2}, ..., v_{i_k}$ with $L^k_{v_{i_1}, v_{i_2}, ..., v_{i_K}}\Lambda$. We remind the definition of the Lie derivative. It is provided by the following two equations:

$$L^0\Lambda = \Lambda, \tag{6}$$

$$L^{k+1}_{v_{i_1},...,v_{i_k},v_{i_{k+1}}}\Lambda = \nabla_S\left(L^k_{v_{i_1},...,v_{i_k}}\Lambda\right)\ .\ v_{i_{k+1}}$$

where the symbol "." denotes the scalar product and ∇_S the gradient operation with respect to the state S. We remark that the Lie derivatives quantify the impact of changes in the control input (u_i) on the output function (h). Now, let us refer to the system in (5) and let us indicate with Ω the space of all the Lie derivatives $L^k_{f_{i_1},...,f_{i_k}}h$, $(i_1, ..., i_k = 1, ..., M)$ and the functions f_{i_j} $(j = (1,\ ...,\ M))$ are defined in (5). Furthermore, we denote with $dL^k_{f_{i_1},...,f_{i_k}}h$ the gradient of the corresponding Lie derivative (i.e. $dL^k_{f_{i_1},...,f_{i_k}}h \equiv \nabla_S L^k_{f_{i_1},...,f_{i_k}}h$) and we denote with $d\Omega$ the space spanned by all these gradients.

In this notation, the observability rank criterion can be expressed in the following way: *The dimension of the largest WLO sub-system at a given S_0 is equal to the dimension of $d\Omega$.*

We now consider again the simple example introduced in section 2 and we show that by using the observability rank criterion we can answer the first question stated in the introduction. In particular, we obtain the same answer already provided in section 2.

The computation of the rank for the system in (3) is straightforward. From the last equation in (3) we obtain: $L^0h = \pi - \theta_R + \phi_R$ whose gradient is $dL^0h \equiv w_1 = [0, -1, 1]$. The first order Lie derivatives are: $L^1_{f_1}h = -\frac{\sin(\theta_R - \phi_R)}{D}$ and $L^1_{f_2}h = 1$. We have: $dL^1_{f_1}h \equiv w_2 = [\frac{\sin(\theta_R - \phi_R)}{D^2}, -\frac{\cos(\theta_R - \phi_R)}{D}, \frac{\cos(\theta_R - \phi_R)}{D}]$. It is easy to realize that each vector w_i obtained by extending the previous computation to every Lie derivative order has the structure: $w_i = [\varrho_i, \varsigma_i, -\varsigma_i]$. Indeed, every Lie derivative will depend on θ_R and ϕ_R only through the quantity $\theta_R - \phi_R$, which changes in sign with respect to the change $\theta_R \leftrightarrow \phi_R$. Therefore, the rank of the matrix

$$\Gamma \equiv \left\{ \begin{array}{c} w_1 \\ ... \\ w_i \\ ... \end{array} \right\} \tag{7}$$

is equal to two. We conclude that the largest WLO sub-system has dimension two as derived in section 2.

3.2 Continuous Symmetries

We refer to the input output system given in (5). We start by remarking that all the available information that we want to use to estimate the state S is contained in the sensor data during a given time interval. Specifically, in the proprioceptive data (used to evaluate the system inputs u) and the exteroceptive data (used to evaluate the system outputs y). On the other hand, the knowledge of the system inputs and outputs in a given time interval is equivalent to the knowledge of all the Lie derivatives at the initial time of the considered interval. This equivalence is at the basis of the theory introduced by Hermann and Krener in [7] and it is a consequence of the two theorems of the implicit functions and the Taylor expansion. Hence, the points in the configuration space where all the Lie derivatives have the same values cannot be distinguished by using the system inputs and outputs collected during a given time interval. For this reason it is fundamental to determine the regions in the configuration space where all the Lie derivatives are invariant. We will call them *indistinguishable regions*. Let us consider the state S_0 in the configuration space. Intuitively speaking, we will call *continuous symmetry* in S_0 a continuous transformation which allows us to determine the associated indistinguishable region (i.e. the region where all the Lie derivatives have the same values as they have in S_0)

In the following we provide respectively a mathematical definition of indistinguishable region and our definition of continuous symmetry. Then, we provide the procedure to determine the indistinguishable regions associated to the continuous symmetries. Finally, we derive theoretical results which play a key role to detect the observable modes for a given input output system. We introduce the following definition:

Definition 1 (Indistinguishable Region) *Given a system described by the eq. in (5), the indistinguishable region (R_{S_0}) associated to a point $S_0 \in \Sigma$ is the largest connected set in Σ, which contains S_0 and the points where all the Lie derivatives have the same value as in S_0.*

As previously mentioned, the points in the configuration space where all the Lie derivatives have the same values cannot be distinguished by using the system inputs and outputs collected during a given time interval. This is the reason because we call these sets indistinguishable regions.

Definition 2 (Continuous Symmetry) *The vector field $w_s(S)$ ($S \in \Sigma$) is a continuous symmetry in S for the system defined in (5) if and only if it is a non null vector belonging to the null space of the matrix whose lines are the gradients of all the Lie derivatives computed in S.*

We now provide the procedure to build an indistinguishable region associated to a given continuous symmetry. Let us consider a point $S_0 \in \Sigma$ and the curve $S(S_0,\ \tau)$ in Σ which is the solution of the differential equation:

$$\begin{cases} \dfrac{dS}{d\tau} = w_s(S) \\ S(0) = S_0 \end{cases} \tag{8}$$

(we assume suitable regularity hypothesis on $w_s(S)$ in order to guarantee the existence of a unique solution).

We prove that the curve $S(S_0,\ \tau)$ is an indistinguishable region of S_0. Before proving this, we prove the following property:

Property 1 *A scalar and differentiable function $g(S)$ $(S \in \Sigma)$ is constant on the curve $S(S_0, \tau)$ if and only if its gradient is orthogonal to $w_s(S)$.*

Proof: Proving this property is immediate. We have: $\frac{dg(S(S_0,\ \tau))}{d\tau} = \nabla_S g\ .\ \frac{dS}{d\tau} = \nabla_S g\ .\ w_s$ ■

Property 2 *The curve $S(S_0,\ \tau)$ which is solution of the differential equation in (8) belongs to the indistinguishable region of S_0.*

Proof: According to the definition 2, w_s is orthogonal to the gradients of all the Lie derivatives. From property 1 we obtain that all the Lie derivatives are constant on the curve $S(S_0,\ \tau)$ ■

It is immediate to extend this result by considering the following differential equation which generalizes the equation in (8) when the system has N_s symmetries $(w_s^1,\ w_s^2, ..., w_s^{N_s})$:

$$\begin{cases} \dfrac{dS}{d\tau} = \displaystyle\sum_{i=1}^{N_s} w_s^i(S)\eta_i(\tau) \\ S(0) = S_0 \end{cases} \tag{9}$$

for every choice of the functions $\eta_1(\tau),\ ...,\ \eta_{N_s}(\tau)$ (provided that the chosen functions guarantee a unique solution for the previous differential equation). The equation in (8) corresponds to the case when all the $\eta_i(\tau)$ are identically 0 with the exception of one of them which is equal to 1.

It also holds the viceversa of property 2, i.e.:

Property 3 *Given S_0, $\forall S \in R_{S_0}$, $\exists$ N_s functions $\eta_1(\tau),\ ...,\ \eta_{N_s}(\tau)$, such that $S = S(S_0, 1)$, where $S(S_0, \tau)$ is the solution of (9).*

Proof: Since R_{S_0} is a connected set, $\forall S \in R_{S_0}$ $\exists$ a curve $S(S_0,\ \tau)$ such that $S(S_0,\ 0) = S_0$ and $S(S_0,\ 1) = S$. Additionally, $S(S_0,\ \tau) \in R_{S_0}\ \forall \tau \in [0, 1]$. Hence, all the Lie derivatives are constant in $S(S_0, \tau),\ \tau \in [0, 1]$. Therefore, the gradient of any Lie derivative is orthogonal to $\frac{dS(S_0,\ \tau)}{d\tau}$ meaning that $\frac{dS(S_0,\ \tau)}{d\tau}$ can be expressed as a linear combination of the continuous symmetries. ■

To better illustrate the previous concepts, we discuss again the simple example provided in section 2.

For the system defined in (3) it exists only one continuous symmetry given by the vector $[0,\ 1,\ 1]^T$ (i.e. belonging to the null space of the matrix Γ in (7)). Let us provide an intuitive interpretation of this continuous symmetry. It is possible to see that this symmetry corresponds to a rotation, which is a global symmetry (independent of S). Indeed, by denoting with $S_0 = [D_0,\ \phi_0,\ \theta_0]^T$, the curve $S(S_0, \tau)$, i.e. the solution of (8), is in this case:

$$\begin{cases} D(\tau) = D_0 \\ \phi(\tau) = \phi_0 + \tau \\ \theta(\tau) = \theta_0 + \tau \end{cases}$$

In other words, the continuous transformation defining this indistinguishable region is the one performing the change $D_0 \rightarrow D_0$, $\phi_0 \rightarrow \phi_0 + \tau$ and $\theta_0 \rightarrow \theta_0 + \tau$ where τ is the continuous parameter characterizing the transformation. On the other hand, the previous transformation corresponds to a rotation of an angle τ. Therefore, this analytical result express what we expected intuitively. Indeed, both the outputs and the inputs for the system in (3) are invariant with respect to a global rotation (see fig. 1).

We now provide the main result in order to deal with real systems and to have an analytical procedure to determine its observable modes. We introduce the following definition:

Definition 3 (Observable Mode) *$g(S)$ is an observable mode if and only if $\forall S_0 \in \Sigma$, $\exists$ a subset U_{S_0} ($S_0 \in U_{S_0}$) such that $R_{S_0} \bigcap \{S \in U_{S_0} | g(S) \neq g(S_0)\} = \emptyset$.*

We have the following property:

Property 4 *$g(S)$ is an observable mode if and only if its gradient is orthogonal to all the symmetries.*

Proof: Let us prove that the gradient of an observable mode is orthogonal to all the symmetries. We proceed by contradiction. Suppose that $\exists\ S_0$ such that $\nabla_S g|_{S_0}\ .\ w_s(S_0) \neq 0$. From the Taylor theorem we have: $g(S(S_0,\ \tau)) = g(S_0) + \nabla_S g|_{S_0}\ .\ w_s(S_0)\ \tau\ +\ o(\tau^2)$. Hence, $\exists\ \tau_M > 0$ such that $\forall\ \tau \in (0,\ \tau_M]$, $g(S(S_0,\ \tau)) \neq g(S_0)$. Since $g(S)$ is an observable mode, $\exists \tau^* \in (0, \tau_M]$ such that the intersection of the set $\{S = S(S_0,\ \tau),\ \tau \in (0,\ \tau^*]\}$ with R_{S_0} must be empty. This last sentence contradicts the result of property 2.

Let us prove the viceversa. If $S \in R_{S_0}$, $S = S(S_0,\ 1)$, where $S(S_0,\ \tau)$ is solution of (9). Since ∇g is orthogonal to all the symmetries, g must be constant on $S(S_0,\ \tau)$ (see property 1). Hence, $g(S) = g(S_0)$. ■

The previous property can be expressed by a system of partial differential equations, one for each symmetry:

$$\sum_{i=1}^{n} w_{si}(S) \frac{\partial g}{\partial S_i} = 0 \tag{10}$$

where $w_{si}(S)$ is the i^{th} component of the symmetry w_s. In other words, for every symmetry there is an associated partial differential equation which must be satisfied by all the observable modes.

We conclude this section by considering the example in section 2. In particular, we use (10) to detect the two observable modes. As previously mentioned, this system has only the symmetry $[0,\ 1,\ 1]^T$. Hence, the associated equation (10) becomes:

$$\frac{\partial g}{\partial \phi_R} + \frac{\partial g}{\partial \theta_R} = 0$$

and two independent solutions are $g = D$ and $g = \theta_R - \phi_R$. This is the same result we obtained in section 2.

4 The Problem of Simultaneous Odometry and Bearing Sensor Calibration

In contrast to the simple example introduced in section 2 where a simple intuitive procedure provides the answers to the theoretical questions stated in the introduction, there are cases where the application of the previous concepts and in particular the use of (10) is required.

Here, we discuss a calibration problem. In this case, the proposed method autonomously derives the observable modes whose physical meaning cannot be found.

4.1 The Considered System

We consider again a mobile robot moving in a $2D$-environment whose dynamics are described by (1). Now we assume that the odometry sensors do not provide directly v and ω. We will consider the case of a differential drive and, in order to characterize the systematic odometry errors, we adopt the model introduced in [5]. We have:

$$v = \frac{r_R\omega_R + r_L\omega_L}{2} \qquad \omega = \frac{r_R\omega_R - r_L\omega_L}{B} \tag{11}$$

where ω_R and ω_L are the control velocities (i.e. $u = [\omega_R,\ \omega_L]^T$) for the right and the left wheel, B is the distance between the robot wheels and r_R and r_L are respectively the radius of the right and the left wheel.

Furthermore, a bearing sensor (e.g. a camera) is mounted on the robot. We assume that its vertical axis is aligned with the $z-$axis of the robot reference frame and therefore the transformation between the frame attached to this sensor and the one of the robot is characterized through the three parameters ϕ, ρ and ψ (see fig. 3).

The available data are the control $u = [\omega_R, \omega_L]^T$ and the bearing angle of a single feature (β in fig. 3) at several time steps during the robot motion.

We introduce the following quantities:

$$\mu \equiv \frac{\rho}{D}; \quad \gamma \equiv \theta + \phi; \tag{12}$$

By using simple trigonometry algebra we obtain (see also fig. 3):

$$\beta = \begin{cases} -atan\left(\dfrac{\sin\gamma}{\mu + \cos\gamma}\right) - \psi + \pi & if\ \gamma_- \leq \gamma \leq \gamma_+ \\ -atan\left(\dfrac{\sin\gamma}{\mu + \cos\gamma}\right) - \psi & otherwise \end{cases}$$

where γ_- and γ_+ are the two solutions (in $[-\pi, \pi)$) of the equation $\cos\gamma = -\mu$ with $\gamma_+ = -\gamma_-$ and $\gamma_+ > 0$. We made the assumption $0 < \mu < 1$ since we want to avoid collisions between the robot and the feature ($D > \rho$).

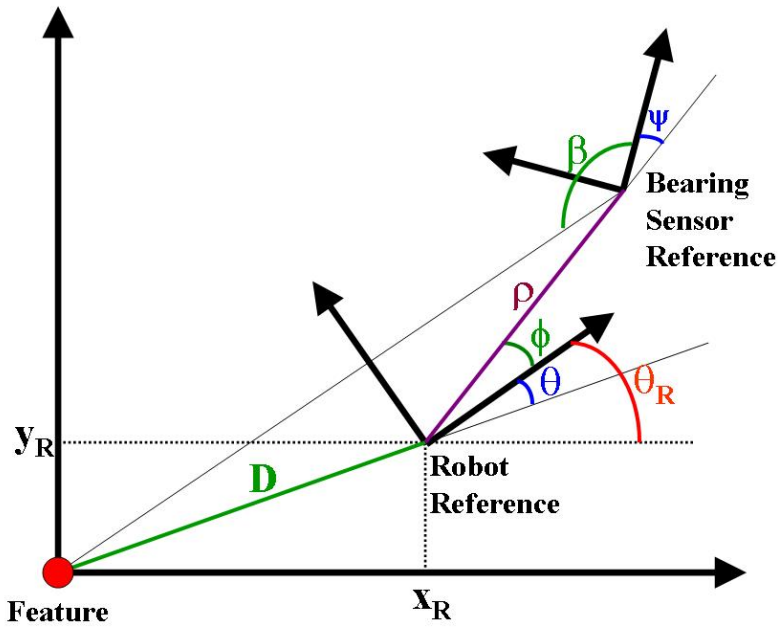

Figure 3: The two reference frames respectively attached to the robot and to the bearing sensor.

By using (1) and the definitions in (12) the dynamics of our system are described by the following equations:

$$\begin{cases} \dot{\mu} = -\mu^2 \dfrac{v}{\rho} \cos(\gamma - \phi) \\ \dot{\gamma} = \omega - \mu \dfrac{v}{\rho} \sin(\gamma - \phi) \\ \dot{\phi} = \dot{\rho} = \dot{\psi} = \dot{r}_R = \dot{r}_L = \dot{B} = 0 \end{cases} \tag{13}$$

The goal is to simultaneously estimate the parameters ϕ, ρ, ψ, r_R, r_L and B by using the available data (i.e. ω_R, ω_L and β in a given time interval). Since these data consist of angle measurements, the best we can hope is the possibility to estimate these parameters up to a scale factor. In other words, the estimation of the four parameters ρ, r_R, r_L and B requires metric information which is not provided by the sensor data. Mathematically, this is a consequence of the fact that we can express both the dynamics and the observation of our system in terms of the following parameters:

$$\phi, \quad \psi, \quad \eta \equiv \frac{r_R}{2\rho}, \quad \delta \equiv \frac{r_L}{r_R}, \quad \xi \equiv \frac{r_R}{B} \tag{14}$$

which are the original angle parameters and suitable ratios of the original parameters which contain metric information (i.e. ρ, r_R, r_L and B). From now on, we will refer to the parameters in (14).

Original Calibration Parameters
Camera: $\phi,\ \rho,\ \psi$ Odometry: $r_R,\ r_L,\ B$
Observable Parameters
$\phi, \quad \psi, \quad \eta \equiv \frac{r_R}{2\rho}, \quad \delta \equiv \frac{r_L}{r_R}, \quad \xi \equiv \frac{r_R}{B}$
Parameters observable in a single q-trajectory
$A^q \equiv \frac{\Psi_1^q - \Psi_3}{1+\Psi_1^q\Psi_3}, V^q \equiv \Psi_2^q \frac{1+\Psi_1^q\Psi_3}{1+\Psi_3^2}, L^q \equiv \psi - atan\Psi_1^q, \xi_q \equiv \xi(1-q\delta)$ where: $\Psi_1^q \equiv \frac{\xi_q - \eta_q \sin\phi}{\eta_q \cos\phi}, \quad \Psi_2^q \equiv \frac{\mu\eta_q \cos\phi}{\sin\gamma}, \quad \Psi_3 \equiv \frac{\mu+\cos\gamma}{\sin\gamma}, \quad \eta_q \equiv \eta(1+q\delta)$

Table 1: Variables adopted in our calibration problem

By using the new parameters in (14) we obtain the following expressions for the dynamics and the observation:

$$\begin{cases} \dot{\mu} = -\mu^2\eta(\omega_R + \delta\omega_L)\cos(\gamma-\phi) \\ \dot{\gamma} = \xi(\omega_R - \delta\omega_L) - \mu\eta(\omega_R + \delta\omega_L)\sin(\gamma-\phi) \\ \dot{\phi} = \dot{\psi} = \dot{\eta} = \dot{\delta} = \dot{\xi} = 0 \\ \beta = \begin{bmatrix} -atan\left(\dfrac{\sin\gamma}{\mu+\cos\gamma}\right) - \psi + \pi & \gamma_- \le \gamma \le \gamma_+ \\ -atan\left(\dfrac{\sin\gamma}{\mu+\cos\gamma}\right) - \psi & otherwise \end{bmatrix} \end{cases} \tag{15}$$

The state $[\mu,\ \gamma,\ \phi,\ \psi,\ \eta,\ \delta,\ \xi]^T$ is WLO as proven in appendix A. On the other hand, to achieve the full observability, the robot must move along all the allowed degrees of freedom (i.e. all the inputs ω_R and ω_L must be considered). In the next subsection we consider circular trajectories (i.e. trajectories characterized by a constant ratio $\frac{\omega_R}{\omega_L}$). For them, the overall system is not WLO. We separate the part of the system which is WLO from the rest by using the theory introduced in section 3.2.

For the sake of clarity we report all the variables adopted in the considered calibration problem in table 1.

4.2 Deriving the Observable Modes for Circular Trajectories

We consider the one-degree of freedom motion obtained by setting

$$\omega_R = \nu; \quad \omega_L = q\nu \tag{16}$$

being q a time-independent parameter (q-trajectory). In this section we focus our attention on a single value of q.

By substituting (16) in (15) we obtain a new system characterized by the same state as in (15) but with a single input (ν) instead of two (ω_R and ω_L). As a result, the weak local observability of the entire state $[\mu,\ \gamma,\ \phi,\ \psi,\ \eta,\ \delta,\ \xi]^T$ is lost: this is proven in appendix B where we prove that the system is even not

weakly observable[1]. We therefore wonder which are the observable modes for the new system.

Intuitively speaking, we must reduce the number of variables to describe our system (i.e. the observation and the dynamics). This is what has been done for the example discussed in section 2 where we reduced the number of variables to describe that system from three to two. The system in (15) is described by seven variables/parameters. It is easy to reduce this number to six by introducing the two parameters:

$$\eta_q \equiv \eta(1 + q\delta) \qquad \xi_q \equiv \xi(1 - q\delta) \tag{17}$$

Indeed, both the observation and the dynamics in (15) can be expressed in terms of $[\mu,\ \gamma,\ \phi,\ \psi,\ \eta_q,\ \xi_q]^T$. In particular, the observation only depends on μ, γ and ψ and the dynamics become:

$$\begin{cases} \dot{\mu} &= -\mu^2 \eta_q \nu \cos(\gamma - \phi) \\ \dot{\gamma} &= \xi_q \nu - \mu \eta_q \nu \sin(\gamma - \phi) \\ \dot{\eta}_q = \dot{\xi}_q = \dot{\phi} = \dot{\psi} &= 0 \end{cases} \tag{18}$$

At this point we wonder if it is possible to further decompose this system (i.e. to further reduce the number of variables/parameters in order to describe the same system). Answering to this question requires to apply the rank criterion, i.e. we need to compute the dimension of the linear space containing the gradients of all the Lie derivatives of the system with the dynamics in (18) and the observation in (15). In the case this rank is equal to 6 (which is the dimension of the vector $[\mu,\ \gamma,\ \phi,\ \psi,\ \eta_q,\ \xi_q]^T$) in at least one point of the space of the states we cannot proceed with the decomposition. In appendix C we prove that this rank is smaller than 6 in any point of the space of states.
In order to further decompose this system we need to adopt the method illustrated in section 3. As we will see, the method is able to introduce autonomously new quantities whose physical meaning cannot be found. Finding a physical meaning for the quantities automatically introduced by the proposed method is equivalent to find an alternative and probably easier procedure able to solve the same problem.

In the next we provide the steps necessary to perform this decomposition. We first consider the following simpler system:

$$\begin{cases} \dot{\mu} &= -\mu^2 \eta_q \nu \cos(\gamma - \phi) \\ \dot{\gamma} &= \xi_q \nu - \mu \eta_q \nu \sin(\gamma - \phi) \\ \dot{\eta}_q = \dot{\xi}_q = \dot{\phi} &= 0 \\ y &= \dfrac{\sin\gamma}{\mu + \cos\gamma} \end{cases} \tag{19}$$

where we removed the variable ψ. The state $[\mu,\ \gamma,\ \phi,\ \eta_q,\ \xi_q]^T$ has dimension equal to 5. On the other hand, the dimension of the linear space containing the gradients of all the Lie derivatives of the system with the dynamics in (19) and the observation in (15) is smaller than 5 (the proof follows the same steps of

[1]We remind that a system which is not weakly observable is certainly not weakly locally observable (WLO); we address the reader to [7] for the definitions of *weak observability* and *weak local observability*.

the proof given in appendix C). By using the matlab symbolic computation it is possible to detect only the following symmetry:

$$w_s = \left[\mu\cos\gamma + 1,\ \sin\gamma,\ \frac{\xi_q\sin\phi - \eta_q}{\mu},\ 0,\ \frac{\xi_q\cos\phi}{\eta_q\mu}\right]^T$$

Since this subsystem is defined by a state whose dimension is five, having one symmetry means that we have four independent observable modes which must satisfy the partial differential equation given in (10) associated to the previous symmetry, i.e.:

$$(\mu\cos\gamma + 1)\frac{\partial\Psi}{\partial\mu} + \sin\gamma\frac{\partial\Psi}{\partial\gamma} + \frac{\xi_q\sin\phi - \eta_q}{\mu}\frac{\partial\Psi}{\partial\eta_q} + \frac{\xi_q\cos\phi}{\eta_q\mu}\frac{\partial\Psi}{\partial\phi} = 0$$

Finding four independent solutions is not difficult since we know that all the Lie derivatives are solutions. However, we need to express the dynamics and the system output through them. Therefore, we cannot use simply the Lie derivatives since their expression is very complicate (with the exception of the zero-order which coincides with the output $\frac{\sin\gamma}{\mu+\cos\gamma}$). On the other hand, a very simple solution for the previous partial differential equation is provided by ξ_q. By using this solution and the output $\frac{\sin\gamma}{\mu+\cos\gamma}$, and starting from the expressions of the first and second order Lie derivatives, we were able to detect two other solutions: $\frac{\xi_q-\eta_q\sin\phi}{\eta_q\cos\phi}$ and $\frac{\mu\eta_q\cos\phi}{\sin\gamma}$. We therefore find the following four independent observable modes:

$$\Psi_1^q \equiv \frac{\xi_q - \eta_q\sin\phi}{\eta_q\cos\phi},\quad \Psi_2^q \equiv \frac{\mu\eta_q\cos\phi}{\sin\gamma},$$

$$\Psi_3 \equiv \frac{\mu+\cos\gamma}{\sin\gamma},\quad \xi_q \tag{20}$$

and the local decomposition of (19) is:

$$\begin{cases} \dot\Psi_1^q = 0 \\ \dot\Psi_2^q = \nu\Psi_2^q(\Psi_1^q\Psi_2^q - \xi_q\Psi_3) \\ \dot\Psi_3 = \nu(\Psi_2^q + \Psi_1^q\Psi_2^q\Psi_3 - \xi_q - \xi_q\Psi_3^2) \\ \dot\xi_q = 0 \\ y = \dfrac{1}{\Psi_3} \end{cases} \tag{21}$$

We now add to the system in (21) the parameter ψ (with $\dot\psi = 0$) and we consider the output $y = \beta = atan\left(\frac{1}{\Psi_3}\right) - \psi$ instead of $y = \frac{1}{\Psi_3}$. In other words we consider our original system described by the new state $[\Psi_1^q,\ \Psi_2^q,\ \Psi_3,\ \xi_q,\ \psi]^T$ whose dimension is five, i.e. smaller than the one of the state $[\mu,\ \gamma,\ \phi,\ \psi,\ \eta_q,\ \xi_q]^T$. We wonder again if we can further proceed with the decomposition. Answering to this question requires to apply the rank criterion to the system satisfying the dynamics in (21) and with the observation $y = \beta = atan\left(\frac{1}{\Psi_3}\right) - \psi$. It is possible to prove that the dimension of the linear space containing the gradients of all the Lie derivatives is always smaller than 5 (which is the dimension of the

vector $[\Psi_1^q,\ \Psi_2^q,\ \Psi_3,\ \xi_q,\ \psi]^T$): the proof is similar to the proof given in appendix C. Therefore, we apply again the method in section 3.

By using the matlab symbolic computation it is possible to detect again a single symmetry:

$$w_s = \left[\Psi_1^{q^2} + 1,\ \Psi_2^q(\Psi_3 - \Psi_1^q)),\ \Psi_3^2 + 1,\ 0,\ 1,\right]^T$$

Since this subsystem is defined by a state whose dimension is five, having one symmetry means that we have four independent observable modes which must satisfy the partial differential equation given in (10) associated to the previous symmetry, i.e.:

$$(\Psi_1^{q^2} + 1)\frac{\partial G}{\partial \Psi_1^q} + (\Psi_2^q(\Psi_3 - \Psi_1^q))\frac{\partial G}{\partial \Psi_2^q} + (\Psi_3^2 + 1)\frac{\partial G}{\partial \Psi_3} + \frac{\partial G}{\partial \psi} = 0$$

namely, every solution $G(\Psi_1^q, \Psi_2^q, \Psi_3, \xi_q, \psi)$ of the previous partial differential equation is a WLO quantity for this resulting system. Again, a very simple solution is provided by ξ_q. Then, by proceeding as before we found the following four independent solutions:

$$A^q \equiv \frac{\Psi_1^q - \Psi_3}{1 + \Psi_1^q\Psi_3}, \qquad V^q \equiv \Psi_2^q\frac{1 + \Psi_1^q\Psi_3}{1 + \Psi_3^2},$$

$$L^q \equiv \psi - atan\Psi_1^q, \qquad \xi_q \tag{22}$$

and the local decomposition is:

$$\begin{cases} \dot{A}^q = \nu(1 + A^{q^2})(\xi_q - V^q) \\ \dot{V}^q = \nu A^q V^q(2V^q - \xi_q) \\ \dot{L}^q = \dot{\xi}_q = 0 \\ \beta\ = -atanA^q - L^q + S_p\dfrac{\pi}{2} \end{cases} \tag{23}$$

where S_p can be ± 1 depending on the values of the system parameters. We do not provide here this dependence. In [16] we derive some important properties relating S_p to the robot motion.

This decomposition has a very practical importance. It tells us that, when the robot accomplishes circular trajectories, the information contained in the sensor data (i.e. the information contained in the function $\nu(t)$ and $\beta(t)$) allows us to estimate only the state $[A^q,\ V^q,\ L^q,\ \xi_q]^T$ and not the original state $[\mu,\ \gamma,\ \phi,\ \psi,\ \xi,\ \delta,\ \eta]^T$. Furthermore, it provides the link between the observable state $[A^q,\ V^q,\ L^q,\ \xi_q]^T$ and the sensor data ν and β. In [16] the previous decomposition has been used to introduce a method which simultaneously calibrates the camera and the odometry system.

5 Aerial Vehicle Equipped with IMU and Camera

In this section we discuss another estimation problem in the framework of the problem of fusing the data provided by a camera and inertial sensors. We adopt

again the concept of continuous symmetry to analytically derive the observable modes.

5.1 The Considered System

Let us consider an aerial vehicle equipped with IMU and a camera. The IMU provides the angular speed and the vehicle acceleration in the local frame attached to this sensor. In particular, we make the assumption that the IMU is offering unbiased measurements. Furthermore, we assume that the configuration of the IMU sensor in the camera frame is perfectly known. Hence, assuming that the vehicle is a rigid body also the camera acceleration is available. We put the local frame attached to the camera. In summary, the IMU provides the angular speed (Ω) and the linear acceleration (A) of the local frame.

We assume that the camera is observing a point feature during a given time interval. We fix a global frame attached to this feature as illustrated in fig 4.

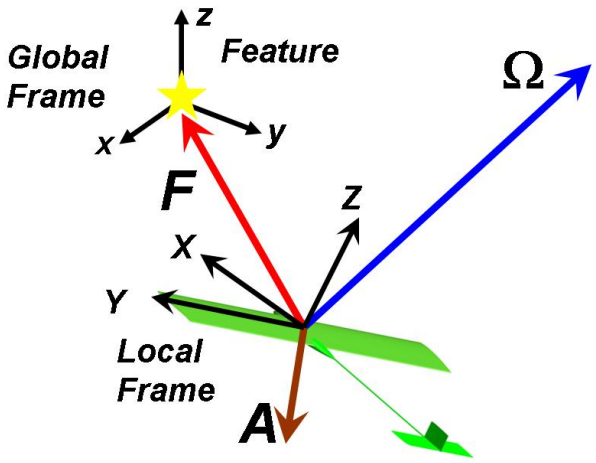

Figure 4: The global and the local frames respectively attached to the feature and the aerial vehicle. The feature position (F), the vehicle acceleration (A) and the vehicle angular speed (Ω) are also displayed.

We will use uppercase letters when the vectors are expressed in the local frame attached to the camera. The same vectors will be indicated with lowercase letters when expressed in the global frame. Finally we will adopt a quaternion to represent the vehicle orientation. Indeed, even if this representation is redundant, it is very powerful since the dynamics can be expressed in a very easy and compact notation.

Our system is characterized by the state $[r,\ v,\ q]^T$ where $r = [r_x,\ r_y,\ r_z]^T$ is the $3D$ vehicle position, v is its time derivative, i.e. the vehicle speed in the global frame ($v \equiv \frac{dr}{dt}$), $q = q_0 + iq_x + jq_y + kq_z$ is a unitary quaternion (i.e. satisfying $q_0^2 + q_x^2 + q_y^2 + q_z^2 = 1$). The analytical expression of the dynamics and the camera observations can be easily provided by expressing all the $3D$ vectors

as imaginary quaternions. In practice, given a $3D$ vector $w = [w_x,\ w_y,\ w_z]^T$ we associate to it the imaginary quaternion $\hat{w} \equiv 0 + iw_x + jw_y + kw_z$. The dynamics of the state $[\hat{r},\ \hat{v},\ q]^T$ are:

$$\begin{cases} \dot{\hat{r}} = \hat{v} \\ \dot{\hat{v}} = q\hat{A}q^* + \hat{a}_g \\ \dot{q} = \frac{1}{2}q\hat{\Omega} \end{cases} \tag{24}$$

being q^* the conjugate of q, $q^* = q_0 - iq_x - jq_y - kq_z$ and $\hat{a}_g$ the imaginary quaternion associated to the gravity acceleration, $a_g \equiv [0\ 0 - g]^T$ with $g \simeq 9.8ms^{-2}$.

In the following, we will consider separately two different cases. In the first one, we assume that the IMU is offering gravity-free measurements. In the second one, this assumption is relaxed. Obviously, the first case is almost unrealistic. On the other hand, considering both the cases allows us to better illustrate the concept of continuous symmetry previously introduced. As we will see, the gravity breaks two of the symmetries which characterize the first case. The dynamics which characterize the first case are characterized by the previous equations by setting the quantity g equal to zero.

We now want to express the camera observations in terms of the same state ($[\hat{r},\ \hat{v},\ q]^T$). We remark that the camera provides the direction of the feature in the local frame. In other words it provides the unit vector $\frac{F}{|F|}$ (see fig. 4). Hence, we can assume that the camera provides the two ratios $y_1 = \frac{F_x}{F_z}$ and $y_2 = \frac{F_y}{F_z}$, being $F = [F_x,\ F_y,\ F_z]^T$. We need to express F in terms of $[\hat{r},\ \hat{v},\ q]^T$. We note that the position of the feature in the frame with the same orientation of the global frame but shifted in such a way that its origin coincides with the one of the local frame is $-r$. Therefore, F is obtained by the quaternion product $\hat{F} = -q^*\hat{r}q$. The observation function provided by the camera is:

$$h_{cam}(\hat{r},\ \hat{v},\ q) = [y_1,\ y_2]^T = \left[\frac{(q^*\hat{r}q)_x}{(q^*\hat{r}q)_z},\ \frac{(q^*\hat{r}q)_y}{(q^*\hat{r}q)_z}\right]^T \tag{25}$$

where the pedix x, y and z indicate respectively the i, j and k component of the corresponding quaternion. We have also to consider the constraint $q^*q = 1$. This can be dealt as a further observation (system output):

$$h_{const}(\hat{r},\ \hat{v},\ q) = q^*q - 1 \tag{26}$$

5.2 Observability Properties for the Case without Gravity

We investigate the observability properties of the system whose dynamics are given in (24) with $g = 0$ and whose observations are given in (25) and (26).

By using the proposed approach it is possible to detect three independent symmetries for this system. They are:

$$w_s^1 = \left[0\ -r_z\ r_y\ 0\ -v_z\ v_y\ -\frac{q_x}{2}\ \frac{q_0}{2}\ -\frac{q_z}{2}\ \frac{q_y}{2}\right]^T \tag{27}$$

$$w_s^2 = \left[r_z\ 0\ -r_x\ v_z\ 0\ -v_x\ -\frac{q_y}{2}\ \frac{q_z}{2}\ \frac{q_0}{2}\ -\frac{q_x}{2}\right]^T$$

$$w_s^3 = \left[-r_y \; r_x \; 0 \; -v_y \; v_x \; 0 \; -\frac{q_z}{2} \; -\frac{q_y}{2} \; \frac{q_x}{2} \; \frac{q_0}{2}\right]^T$$

These symmetries could also be derived by remarking the system invariance with respect to rotations about all the three axes. For instance, an infinitesimal rotation of magnitude ϵ about the vertical axis changes the state as follows [6]:

$$\begin{bmatrix} r_x \\ r_y \\ r_z \end{bmatrix} \rightarrow \begin{bmatrix} r_x \\ r_y \\ r_z \end{bmatrix} + \epsilon \begin{bmatrix} -r_y \\ r_x \\ 0 \end{bmatrix}$$

$$\begin{bmatrix} v_x \\ v_y \\ v_z \end{bmatrix} \rightarrow \begin{bmatrix} v_x \\ v_y \\ v_z \end{bmatrix} + \epsilon \begin{bmatrix} -v_y \\ v_x \\ 0 \end{bmatrix}$$

$$\begin{bmatrix} q_0 \\ q_x \\ q_y \\ q_z \end{bmatrix} \rightarrow \begin{bmatrix} q_0 \\ q_x \\ q_y \\ q_z \end{bmatrix} + \frac{\epsilon}{2} \begin{bmatrix} -q_z \\ -q_y \\ q_x \\ q_0 \end{bmatrix}$$

that is:

$$\begin{bmatrix} r \\ v \\ q \end{bmatrix} \rightarrow \begin{bmatrix} r \\ v \\ q \end{bmatrix} + \epsilon w_s^3$$

On the other hand, without applying the method introduced in section 3 we could not conclude that the previous ones are *all* the symmetries for the considered system.

We remark that for every symmetry there is an associated partial differential equation (the one provided in (10)). Hence, every WLO quantity must satisfy simultaneously all the three partial differential equations. Since our system is defined by 10 variables, the number of independent solutions satisfying all the three partial differential equations is $10 - 3 = 7$ [10]. On the other hand, their derivation, once the three symmetries are detected, is pretty easy. Indeed, it is immediate to prove that the distance of the feature from the camera, i.e. $|r|$, is a solution of the three equations (this can be checked by substitution for the partial differential equations associated to the symmetries in (27) but can also proved by remarking that the scale factor is invariant under rotations). This means that the distance of the feature is observable and it is one among the 7 independent solutions.

On the other hand, since the camera provides the position of the feature in the local frame up to a scale factor, having the distance means that the feature position in the local frame is also observable. Therefore the three components of the feature position in the local frame are three independent solutions. By using quaternions we can say that three independent solutions are provided by the components of the imaginary quaternion $q^* \hat{r} q$. Furthermore, since the three partial differential equations are invariant under the transformation $r \leftrightarrow v$ (again this can be checked for partial differential equation associated to the first symmetry in (27)), three other independent solutions are the components of the imaginary quaternion $q^* \hat{v} q$. Physically, this means that the vehicle speed in the local frame is also observable. Finally, the last solution is $q^* q$ since it is directly

observed (see equation (26); it can be in any case verified that it satisfies the three partial differential equations).

5.3 Observability Properties for the Case with Gravity

We investigate the observability properties of the system whose dynamics are given in (24) with $g \neq 0$ and whose observations are given in (25) and (26).

The presence of the gravity breaks two of the previous three symmetries. In other words, the system remains invariant only with respect to rotations about the vertical axis. This means that w_s^1 and w_s^2 are not symmetries for the new system while w_s^3 it is. On the other hand, we cannot conclude that w_s^3 is the only symmetry for the system. In order to derive all the symmetries we need to directly use the definition 2. By computing the Lie derivatives up to the third order we were able to conclude that the system has a single symmetry.

The partial differential equation associated to w_s^3 is:

$$\begin{aligned} -2r_y\frac{\partial\Lambda}{\partial r_x} + 2r_x\frac{\partial\Lambda}{\partial r_y} - 2v_y\frac{\partial\Lambda}{\partial v_x} + 2v_x\frac{\partial\Lambda}{\partial v_y} + \\ -q_z\frac{\partial\Lambda}{\partial q_t} - q_y\frac{\partial\Lambda}{\partial q_x} + q_x\frac{\partial\Lambda}{\partial q_y} + q_t\frac{\partial\Lambda}{\partial q_z} = 0 \end{aligned} \tag{28}$$

The number of independent solutions $\Lambda = \Lambda(r_x,\ r_y,\ r_z,\ v_x,\ v_y,\ v_z,\ q_t,\ q_x,\ q_y,\ q_z)$ is equal to the number of variables (i.e. 10) minus the number of equations (i.e. 1) [10]. Hence in this case we have two additional observable modes. These modes can be derived by using classical methods to solve partial differential equations [10]. They are:

$$Q_r \equiv \frac{q_t q_x + q_y q_z}{1 - 2(q_x^2 + q_y^2)}; \qquad Q_p \equiv q_t q_y - q_z q_x \tag{29}$$

Also for these two solutions it is possible to find a physical meaning. They are related to the two angles: roll and pitch [12]. In particular, the first solution provides the roll angle which is $R = \arctan(2Q_r)$. The latter provides the pitch angle which is $P = \arcsin(2Q_p)$.

6 Local Decomposition and Estimation based on an EKF

In this section we consider again the system discussed in the previous section. We separate the observable modes from the rest of the system. In other words, we write the dynamics of the observable modes only in terms of themselves and we also express the observations in terms of the same observable modes. This decomposition will allow us to implement an Extended Kalman Filter in order to perform the estimation of the observable modes. We will provide the system decomposition for the two cases, i.e. with and without gravity.

6.1 The Case Without Gravity

Separating the observable modes from the rest of the system is pretty trivial. Regarding the quaternion, which describes the vehicle orientation, we know

that, apart the fact the is norm is 1, it is not observable. Therefore, it must be possible to separate the quaternion from the observable modes. Starting from the equations (24) we can write the dynamics for the vectors F and V (defined in section 5.1). We have:

$$\begin{cases} \dot{F} = MF - V \\ \dot{V} = MV + A \end{cases} \tag{30}$$

where the two matrices M and m depend on the angular speed:

$$M \equiv \begin{bmatrix} 0 & \Omega_z & -\Omega_y \\ -\Omega_z & 0 & \Omega_x \\ \Omega_y & -\Omega_x & 0 \end{bmatrix}$$

$$m \equiv \frac{1}{2} \begin{bmatrix} 0 & -\Omega_x & -\Omega_y & -\Omega_z \\ \Omega_x & 0 & \Omega_z & -\Omega_y \\ \Omega_y & -\Omega_z & 0 & \Omega_x \\ \Omega_z & \Omega_y & -\Omega_x & 0 \end{bmatrix}$$

Regarding the observation function given in (25), its expression in terms of F is very easy:

$$h_{cam}(\hat{r},\ \hat{v},\ q) = [y_1,\ y_2]^T = \left[\frac{F_x}{F_z},\ \frac{F_y}{F_z}\right]^T \tag{31}$$

By discretizing the equations in (30) and by computing the Jacobians (also of the observation in (31)) it is possible to implement the standard EKF equations.

6.2 The Case With Gravity

In this case separating the observable modes from the rest of the system is more complex since the roll and the pitch angles are observable. It is clearly possible to write:

$$\begin{cases} \dot{F} = MF - V \\ \dot{V} = MV + A + A_g \end{cases} \tag{32}$$

being A_g the gravity acceleration in the local frame, i.e. $\hat{A}_g = q^* \hat{a}_g q$. Instead of considering the two modes defined in (29), we found easier to characterize the observable part of the vehicle orientation by the following two independent observable modes:

$$m_1 = \frac{q_x^2 + q_y^2}{q_0 q_y - q_x q_z} \qquad m_2 = \frac{q_x^2 + q_y^2}{q_0 q_x + q_y q_z} \tag{33}$$

The dynamics of these modes are:

$$\begin{cases} \dot{m}_1 = \Omega_x \dfrac{m_1}{m_2} + \dfrac{\Omega_y}{2}\left(m_1^2 + 1 - \dfrac{m_1^2}{m_2^2}\right) + \Omega_z \dfrac{m_1^2}{m_2} \\ \dot{m}_2 = \dfrac{\Omega_x}{2}\left(m_2^2 - \dfrac{m_2^2}{m_1^2} + 1\right) + \Omega_y \dfrac{m_2}{m_1} - \Omega_z \dfrac{m_2^2}{m_1} \end{cases} \tag{34}$$

In order to complete the system decomposition we have to express the quaternion q which appears in (32) through the term A_g only in terms of m_1 and m_2.

The expression of the quaternion in terms of the roll, pitch and yaw angles is [12]:

$$\begin{aligned} q = CrCpCy + SrSpSy + i(SrCpCy - CrSpSy) + \\ +j(CrSpCy + SrCpSy) + k(CrCpSy - SrSpCy) \end{aligned} \tag{35}$$

where r, p and y denote respectively the roll, pitch and yaw angles and C and S the cosinus and sinus functions (e.g. Cr is $\cos(r)$).

We remind that A_g is the gravity in the local frame. On the other hand, rotating the gravity around the vertical axis does not affect the expression of A_g. For this reason, we set the yaw angle equal to zero. The experssion of the quaternion becomes:

$$q = CrCp + iSrCp + jCrSp - kSrSp \tag{36}$$

Finally, we express the angles r and p in terms of m_1 and m_2:

$$\begin{aligned} r &= atan\left(\frac{m_1^2 m_2}{m_1^2 + m_2^2 - m_1^2 m_2^2}\right) \\ p &= asin\left(\frac{2m_1 m_2^2}{m_1^2 + m_2^2 + m_1^2 m_2^2}\right) \end{aligned} \tag{37}$$

The equations (32), (34), (36) and (37) provide the dynamics of the observable modes. Regarding the observation function, the expression is still the one given in (31).

As in the previous case, these analytical expressions allow us to implement an EKF to perform the estimation of the observable state $[F,\ V,\ m_1,\ m_2]^T$.

7 Performance Evaluation

In this section we propose several simulations and experiments in order to prove the importance of the theory developed in section 3 and its applications discussed in the sections 4, 5 and 6.

We start by performing simulations for the simple system introduced in section 2. In particular, we compare the results achievable by estimating the non observable state and by estimating the observable modes. We repeat the same analysis for the system discussed in section 5. Finally, regarding the calibration problem discussed in section 4 the results are available in [16].

7.1 Simulations for the System defined in Section 2

We simulate a differential drive mobile robot moving in a $2D$ environment. The dynamics of the simulated robot are described by the equations (1) where $v = \frac{v_R + v_L}{2}$ and $\omega = \frac{v_R - v_L}{w_b}$ and v_R, v_L are respectively the speed of the right and left wheel and w_b is the distance between them. The motion is generated by randomly setting v_R and v_L at each time step of $0.01s$. The robot is equipped with encoder sensors able to provide the shift of the right and the left wheel

occurred at every time step. These encoder data are delivered at $100Hz$. Furthermore, accordingly to the model introduced in [5], all these measurements are affected by zero mean Gaussian errors independent among them. In particular, according to the error model in [5], the variance of each measurement is proportional to the value provided by the sensor. In other words, let us suppose that the true shift of the right wheel occurred at a given time step is equal to δ_R^{true}. We generate the measurement $\delta_R = N\left(\delta_R^{true}, K^2|\delta_R^{true}|\right)$, being $N(m, \sigma^2)$ the normal distribution with mean value m and variance σ^2 and K characterizes the non systematic odometry error. We considered many different values for the parameter K. In the simulations here provided we set $K = 0.1m^{\frac{1}{2}}$.

The simulated exteroceptive sensor provides the bearings of a single feature at the origin. These data are delivered at $1Hz$. Furthermore, we assume that these bearing measurements are affected by a zero mean Gaussian error. In other words, when at a given time step the true bearing is β^{true} we generate the measurement $\beta = N(\beta^{true}, \sigma_\beta^2)$. In the simulations here provided we set $\sigma_\beta = 10\ deg$.

Figure 5 shows the true trajectory (blue dots) and the trajectory estimated by using an EKF (green circles). As expected the estimated state is affected by a drift.

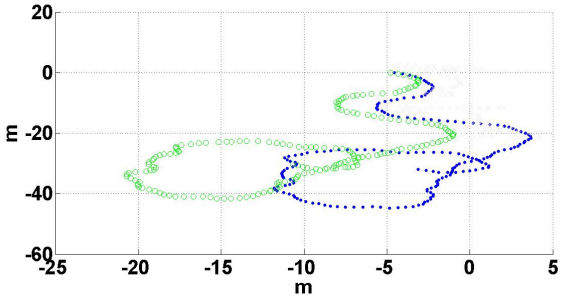

Figure 5: The true trajectory (blue dots) and the trajectory estimated by using an EKF (green circles).

Figure 6 shows the distance of the robot from the origin vs time (in s). The true distances are displayed with blue dots. The green circles display the value of the distances obtained from the values of x and y shown in figure 5. Finally, the black crosses show the distances estimated by implementing an EKF which estimates the observable modes, i.e. the state $[D,\ \theta]^T$ (the equations of this EKF can be obtained by discretizing the equations in (4)). We remark that in both cases there is no drift on the estimated distances.

We have performed many simulations obtaining similar results. Therefore, regarding this simple example we can conclude with the following remarks:

1. The estimation of the non-observable state ($[x,\ y,\ \theta]^T$) is affected by a drift;
2. The observable modes obtained from the estimates of the previous non-observable state are not affected by a drift;
3. The observable modes directly estimated by an EKF are not drift-affected;

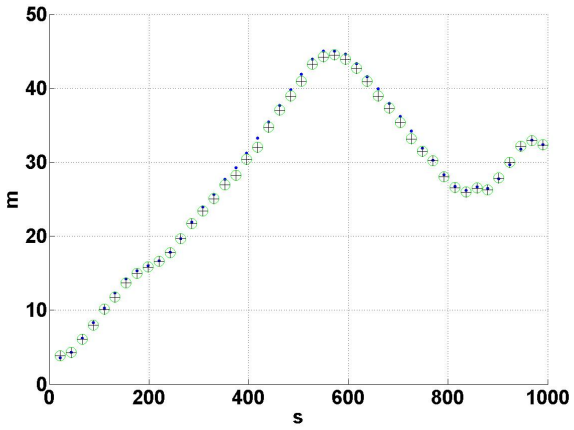

Figure 6: The true distances (blue dots), the value of the distances obtained from the values of x and y shown in figure 5 (green circles) and the distances estimated by implementing an EKF which directly estimates the observable modes (black crosses).

4. Obtaining the observable modes from the non-observable state or directly estimating them with an EKF is equivalent in terms of precision.

We will see that the last remark does not hold in the example considered in section 5. Therefore, it is in general fundamental not only detecting the observable modes but also to separate them from the rest of the system.

7.2 Simulations for the System defined in Section 5

We simulate an aerial vehicle which moves along random trajectories in $3D$. The trajectory is generated by generating randomly the linear and angular acceleration at 100 Hz. In particular, at each time step, the three components of the linear and the angular acceleration are generated as zero-mean Gaussian independent variables with variance respectively equal to $\left(1\ \frac{m}{s^2}\right)^2$ and $\left(1\ \frac{deg}{s^2}\right)^2$. We adopt many different values for the initial vehicle speed and position. Starting from the accomplished trajectory, the true angular speed and the linear acceleration are computed at each time step of $0.01s$ (respectively, at the time step i, we denote them with Ω_i^{true} and A_i^{true}). Starting from them, the IMU sensors are simulated by generating randomly the angular speed and the linear acceleration at each step according to the following: $\Omega_i = N\left(\Omega_i^{true}, P_{\Omega_i}\right)$ and $A_i = N\left(A_i^{true}, P_{A_i}\right)$ where P_{Ω_i} and P_{A_i} are the covariance matrices characterizing the accuracy of the IMU. In the simulations we set both these matrices to diagonal matrices and their components are such that the accuracy of the sensor is 5% (for instance, for generating the x component of A_i (i.e. $A_{i\ x}$), the first element on the diagonal of P_{A_i} is set equal to $\left(0.05\ A_{i\ x}^{true}\right)^2$).

Regarding the camera, the provided readings are generated randomly in the following way. By knowing the true trajectory, the true bearing angles of the feature (at the origin) in the camera frame are computed. They are computed

each $0.2s$. Then, the camera readings are generated by adding to the true values zero-mean Gaussian errors whose variance is equal to $(1\ deg)^2$ for all the readings.

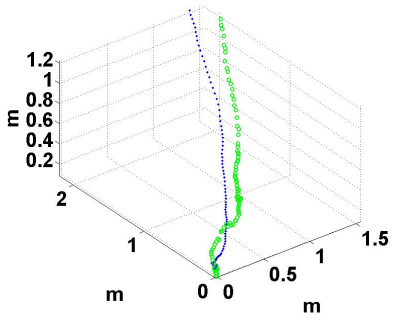

Figure 7: Results from the EKF which estimates the entire non-observable state. The $3D$ trajectory is displayed. The blue dots indicate the ground truth while the green circles the estimated trajectory.

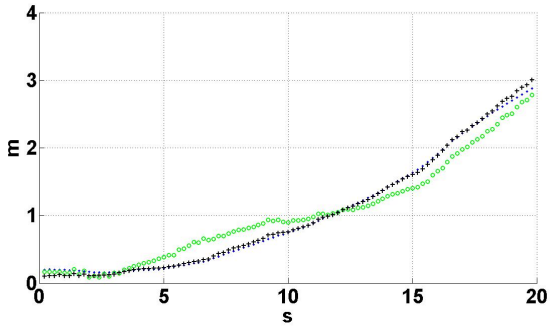

Figure 8: The true distances (blue dots), the value of the distances obtained from the values of x, y and z shown in figure 7 (green circles) and the distances estimated by implementing an EKF which directly estimates the observable modes (black crosses).

We performed many simulations. Figures 7 and 8 show the typical results we obtained from them. In fig 7 the $3D$ trajectory is displayed. The blue dots indicate the ground truth while the green circles the trajectory estimated by implementing an EKF which estimates the non-observable state $[r,\ v,\ q]^T$. As expected, the estimation is affected by a drift. Fig 8 displays the distance of the vehicle from the origin vs time. Blue dots indicate the true values, green circles the values obtained from the values of x, y and z shown in figure 7 and black crosses indicate the distances estimated by implementing an EKF which directly estimates the observable modes (i.e. the state $[F,\ V,\ m_1,\ m_2]^T$).

We performed many simulations obtaining similar results. We conclude with the following remarks:

1. The estimation of the non-observable state ($[r,\ v,\ q]^T$) is affected by a drift;
2. The estimation of the observable modes obtained from the estimates of the previous non-observable seems to be not affected by a drift;
3. The observable modes directly estimated by an EKF are not drift-affected;
4. Directly estimating the observable modes is much more convenient than obtaining them from the non-observable state in terms of precision.

8 Conclusions

In this paper we considered the problem of estimation in autonomous navigation from a theoretical perspective. In particular, the investigation regarded problems where the information provided by the sensor data is not sufficient to carry out the state estimation (i.e. the state is not observable). In order to properly exploit the information in the sensor data, it is necessary to separate the observable part of the system from the rest. In this paper we used the concept of continuous symmetry to achieve this goal. We illustrated this concept by providing a very simple example. Then, we apply the same concept to derive the observable modes for more complex systems. In these cases, the concept of continuous symmetry played a key role in detecting how the information contained in the sensor data is related to the observable modes. It is interesting to note that the method is able to derive autonomously the observable modes without the need of knowing their physical meaning. In this sense, the calibration problem better shows the importance of the concept of continuous symmetry. Indeed, in this case the modes automatically introduced do not have physical meaning (or at least it seems impossible to find it).

The importance of the proposed concept has been illustrated by showing how it can improve the estimation performance in the considered systems.

Acknowledgment

This work was supported by the European Commission FP7-ICT-2007-3.2.2 Cognitive Systems, Interaction, and Robotics under the contract #231855 (sFLY).

A Observability for the system defined by equation (15)

Let us refer to the system whose dynamics and observation are defined in (15). In order to prove that it is WLO, according to the rank criterion, we provide seven Lie derivatives whose gradients span the entire configuration space. Let us consider the matrix whose lines are the gradients of the Lie derivatives: $L^0\beta$, $L^1_{f_1}\beta$, $L^1_{f_2}\beta$, $L^2_{f_1f_1}\beta$, $L^2_{f_1f_2}\beta$, $L^2_{f_2f_1}\beta$ and $L^2_{f_2f_2}\beta$, where $f_1 = -\left[\mu^2\eta\cos(\gamma-\phi), \mu\eta\sin(\gamma-\phi)-\xi, 0, 0, 0, 0, 0\right]^T$ and $f_2 = -\delta\left[\mu^2\eta\cos(\gamma-\phi), \mu\eta\sin(\gamma-\phi)+\xi, 0, 0, 0, 0, 0\right]^T$. The determinant of this matrix is: $-16\delta^4\mu^5\eta^3\xi^5\cos(\gamma-\phi)(\mu\cos\phi-\cos(\gamma-\phi))/(\mu^2+2\mu\cos\gamma+1)^5$ which is different from 0 with the exception of the points where one of the following conditions is satisfied: $\mu\cos\phi = \cos(\gamma-\phi)$, $\gamma = \phi + j\frac{\pi}{2}$ (j being an integer). By indicating with Θ this set of points we remark that its interior is empty (i.e. for every $S \in \Theta$, every open ball centered in S contains at least one point outside Θ). Starting from this fact and by analyzing the dynamics in (15) it is possible to find a control able to move the state outside Θ instantaneously.

B Non weak observability for the system defined by equation (15) with the constraint on its input given in (16)

Let us refer to the system whose dynamics and observation are defined in (15) with the single input ν according to the constraint given in (16). We will show that there are infinite initial states which cannot be distinguished.

Let us consider the initial state $S^0 \equiv [\mu^0,\ \gamma^0,\ \phi^0,\ \psi^0,\ \eta^0,\ \delta^0,\ \xi^0]^T$. All the initial states $S(\lambda) \equiv \left[\mu^0,\ \gamma^0,\ \phi^0,\ \psi^0,\ \frac{\eta^0(1+q\delta^0)}{1+q\lambda},\ \lambda,\ \frac{\xi^0(1-q\delta^0)}{1-q\lambda}\right]^T$ (being $\lambda \in \Re^+$) provides the same output (β) for any choice of the input ν. Indeed, the output in (15) only depends on μ, γ and ψ whose dynamics are independent of λ. This proves the non observability of the considered system. On the other hand, when $\lambda \to \delta^0$ $S(\lambda) \to S^0$. Hence, even states which are close to S_0 cannot be distinguished from S_0. Therefore, the system is not weakly observable according to the definition of weak observability given in [7].

C Observability rank criterion for the system with the dynamics in (18) and the observation in (15)

According to the observability rank criterion, we need to calculate the dimension of the linear space containing the gradients of all the Lie derivatives of the observation function in (15) along the dynamics given in (18). On the other hand, since our system is affine in the input, we can restrict the computation to the first $n-1$ Lie derivatives, being n the dimension of the state $[\mu,\ \gamma,\ \phi,\ \psi,\ \eta_q,\ \xi_q]^T$, i.e. $n = 6$ and $n-1 = 5$ (see [1], chapter 4). By a direct computation carried out with the help of the matlab symbolic tool, we obtain that the determinant

of the matrix whose lines are the gradients of the first five Lie derivatives and the observation function (which is the zero order Lie derivative) is equal to zero in any point of the space of the states. Therefore, the dimension of the linear space containing the gradients of all the Lie derivatives is always smaller than 6.

References

[1] Anguelova M., Non linear Observability and Identifiability: General Theory and a Case Study of a Kinetic Model, PhD thesis, Goteborg, April 2004

[2] Bicchi A., Pratichizzo D., Marigo A. and Balestrino A., On the Observability of Mobile Vehicles Localization, IEEE Mediterranean Conference on Control and Systems, 1998

[3] Bonnifait P. and Garcia G., Design and Experimental Validation of an Odometric and Goniometric Localization System for Outdoor Robot Vehicles, IEEE Transaction On Robotics and Automation, Vol 14, 1998

[4] Brogan W. L. Modern Control Theory, 3rd ed. Englewood Cliffs, NJ: Prentice Hall, 1991

[5] Chong K.S., Kleeman L., "Accurate Odometry and Error Modelling for a Mobile Robot," *International Conference on Robotics and Automation*, vol. 4, pp. 2783–2788, 1997.

[6] Goldstein, H. Classical Mechanics, 2nd ed. Reading, MA: Addison-Wesley, 1980

[7] Hermann R. and Krener A.J., 1977, Nonlinear Controllability and Observability, IEEE Transaction On Automatic Control, AC-22(5): 728-740

[8] Huang G.P., Mourikis A.I., and Roumeliotis S.I., "Analysis and improvement of the consistency of extended Kalman filter based Slam", In Proceedings of the 2008 IEEE International Conference on Robotics and Automation (ICRA), pages 473479, May 2008.

[9] Isidori A., Nonlinear Control Systems, 3rd ed., Springer Verlag, 1995.

[10] F. John, Partial Differential Equations, Springer-Verlag, 1982.

[11] Kosut R.L., Arbel A. and Kessler K.M., Optimal Sensor System Design for State Reconstruction, IEEE Tran Aut Cont., Vol 27, 1982

[12] Quaternions and rotation Sequences: a Primer with Applications to Orbits, Aerospace, and Virtual Reality. Kuipers, Jack B., Princeton University Press copyright 1999.

[13] Lee K. W., Wijesoma W. S. and Guzman J.I., On the Observability and observability analysis of SLAM. In Proceedings of IEEE International Conference on Intelligent Robots and Systems, Benjing, China, 2006.

[14] Lorussi F, Marigo A. and Bicchi A., Optimal exploratory paths for a mobile rover, IEEE International Conference on Robotics and Automation (ICRA), 2001, Vol 2, Pages:2078 - 2083

[15] Martinelli A., Scaramuzza D. and Siegwart R., Automatic Self-Calibration of a Vision System during Robot Motion, International Conference on Robotics and Automation, Orlando, Florida, April 2006.

[16] Martinelli A., Using the Distribution Theory to Simultaneously Calibrate the Sensors of a Mobile Robot, Internal Research Report, INRIA, http://hal.inria.fr/inria-00353079/en/

[17] Mirzaei F.M. and Roumeliotis S.I., A Kalman filter-based algorithm for IMU-camera calibration: Observability analysis and performance evaluation, IEEE Transactions on Robotics, 2008, Vol. 24, 2008

[18] Perera L., Wijesoma W.S. and Adams M., The Estimation Theoretic Sensor Bias Correction Problem in Map Aided Localization, International Journal of Robotics Research, Vol 25, Issue 7, July 2006.

[19] The Rawseeds Project http://www.rawseeds.org/home/

[20] Roumeliotis S.I. and Bekey G.A., 2002, Distributed Multirobot Localization, IEEE Transaction On Rob and Aut Vol 18

Contents

Centre de recherche INRIA Grenoble – Rhône-Alpes
655, avenue de l'Europe - 38334 Montbonnot Saint-Ismier (France)

Centre de recherche INRIA Bordeaux – Sud Ouest : Domaine Universitaire - 351, cours de la Libération - 33405 Talence Cedex
Centre de recherche INRIA Lille – Nord Europe : Parc Scientifique de la Haute Borne - 40, avenue Halley - 59650 Villeneuve d'Ascq
Centre de recherche INRIA Nancy – Grand Est : LORIA, Technopôle de Nancy-Brabois - Campus scientifique
615, rue du Jardin Botanique - BP 101 - 54602 Villers-lès-Nancy Cedex
Centre de recherche INRIA Paris – Rocquencourt : Domaine de Voluceau - Rocquencourt - BP 105 - 78153 Le Chesnay Cedex
Centre de recherche INRIA Rennes – Bretagne Atlantique : IRISA, Campus universitaire de Beaulieu - 35042 Rennes Cedex
Centre de recherche INRIA Saclay – Île-de-France : Parc Orsay Université - ZAC des Vignes : 4, rue Jacques Monod - 91893 Orsay Cedex
Centre de recherche INRIA Sophia Antipolis – Méditerranée : 2004, route des Lucioles - BP 93 - 06902 Sophia Antipolis Cedex

Éditeur
INRIA - Domaine de Voluceau - Rocquencourt, BP 105 - 78153 Le Chesnay Cedex (France)
http://www.inria.fr
ISSN 0249-6399